Status of the Eltrap Project

M. Amoretti*, G. Bettega*, F. Cavaliere*, M. Cavenago†, F. De Luca*, R. Pozzoli* and M. Romé*

*I.N.F.M. (U.d.R. Milano Università) and Dipartimento di Fisica, Università degli Studi di Milano, Via Celoria 16, 20133 Milano, Italy
†I.N.F.N. Laboratori Nazionali di Legnaro, via Romea 4, 35020 Legnaro, Italy

Abstract. The Malmberg-Penning trap Eltrap recently installed at the University of Milano, features a magnetic field with a high degree of uniformity in a relatively large plasma volume, and an enhanced light collection by the CCD camera. A modular electrode design allows several variations of the experimental configuration, suitable both for electron confinement and beam studies. The major electronic components of the apparatus are a waveform generator, which controls the inject-hold-dump cycle, and two personal computers, which control the data acquisition, the setting, and the timing of the experiments. Different electron sources have been proposed for the project, and studies for advanced source production are in progress.

INTRODUCTION

The Eltrap machine recently installed at the University of Milano is a Malmberg-Penning trap, with a magnetic field up to 0.2 T, and equipped with a CCD optical diagnostics. It is intended to be a small scale facility for electron plasma and beam dynamics experiments, and in particular for the study of collective effects, equilibrium states, and formation of coherent structures in these systems [1, 2, 3, 4, 5]. Its versatility should also allow different operational regimes [6].

The general scheme of Eltrap is shown in Fig. 1. Several characteristics are similar to those of the EV and CamV devices at UCSD [7, 8], its major limitation being the magnetic field strength. The machine can be also viewed as a scaled version (higher as linear dimensions, lower as for current and voltages) of several devices used in accelerator physics, as, e.g., Electron Beam Ion Sources or einzel lenses. In Eltrap, a magnetic field with a very high uniformity in a relatively large plasma volume has been designed and obtained (also by means of a careful placement of iron shims and the use of dipole correcting coils). The light collection is optimized by mounting the viewport on a reentrant flange, as shown in Fig. 1. The electronic control and acquisition systems are fully based on personal computers, and show some novelties concerning interfaces and pulse generation with respect to the solutions adopted in similar devices. Studies on different electron sources are in progress.

CP606, *Non-Neutral Plasma Physics IV*, edited by F. Anderegg et al.

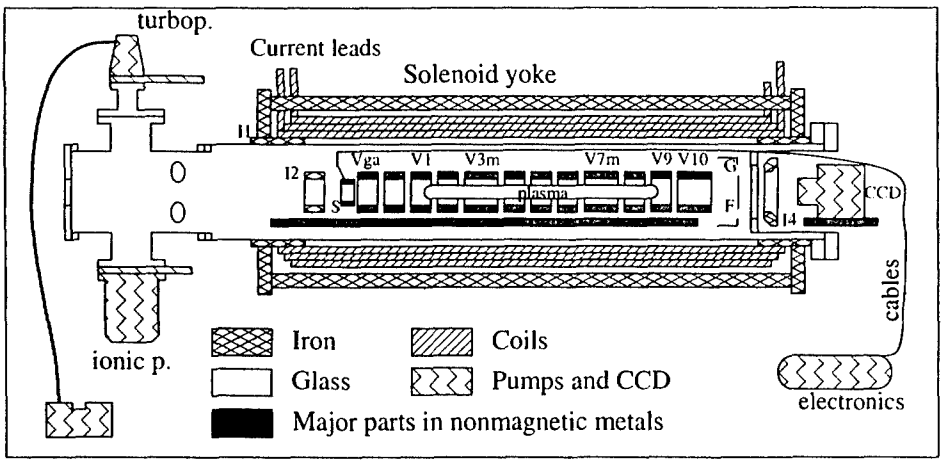

FIGURE 1. Scheme of the Eltrap machine.

DESIGN AND DESCRIPTION OF THE APPARATUS

The vacuum chamber of Eltrap is a 1.75 m long stainless steel tube with an outer diameter of 256 mm. The solenoid is 1.5 m long, with an inner diameter $D = 320$ mm. The gap between the vacuum tube and the magnet is available for the bakeout system, alignment purposes, and/or additional quadrupole windings.

The main requirement in the design of the magnet was to obtain a uniform field over a length $L \cong 1$ m, in the central region close to the axis. To this aim, a minimal coil length $L_1 = L + f_1 D$ is necessary (with $f_1 \cong 4/3$ for a stack of pancake coils). The practical need of wire connection requires that the end of the coil is tapered for a length $L_2 \cong 4$ cm. Since this can be detrimental to field uniformity, the coil has been made longer (length $L_3 = L + f_1 D + 2L_2$) and a 1 cm thick iron ring has been inserted inside each coil end (shims I1 and I3). Two additional truncated conical shims (I2 and I4) are used to further improve the field uniformity, since their presence concentrates the field lines towards the axis. Extensive numerical computations have been used to complete the magnet and shim design, giving a uniformity better than 10^{-3} within a distance of 0.5 m from the center of the magnet. In addition, the solenoid is enclosed in a soft iron cage made by two square end-plates and 12 axial bars: this simplifies the support system, and represents also a shield against the Earth's magnetic field. Both analytical estimates and numerical computations excluded the presence of a dodecapole field in the plasma over a 5×10^{-5} level.

The solenoid coil consists of three helical winding layers: this design has been chosen to avoid wire transposition in the coil central region. Each winding layers is trifilar. The nine conductors are water cooled in parallel and electrically connected in series. Four dipole correcting coils compensate errors in the main solenoid winding. The solenoid current is generated and controlled by a highly stabilized power supply ($dI/dt = 10^{-5}$ per hour, $V \leq 120$ V, $I \leq 600$ A).

The phosphor screen F is placed at a distance $\cong L_3/2 - D/2$ from the center of the magnet, inside the region of almost uniform magnetic field, in order to avoid image distorsion effects. Placing the CCD camera close to phosphor screen is also beneficial, since the solid angle for light collection is $\Omega_1 = \pi d_l^2/(4p^2)$, where p is the distance between F and the lens, and d_l is the diameter of the lens. To reduce p, a reentrant flange is used. This has also mechanical advantages: the shim I4 remains in air, and the phosphor screen can be sustained directly on the flange. This design allows $p \geq 100 \div 110$ mm and $\Omega_1 \leq 0.05$ sr. In order to get the desired magnification factor, $M = q/p > s_c/D = 0.28$, where $s_c = 25$ mm is the side of the CCD sensor, the distance q between the lens and the CCD sensor should be in the range $[51, 76]$ mm. The operational ranges of the different parameters are: $q \in [64, 76]$ mm, $M \in [0.28, 0.52]$, $p \in [146, 230]$ mm, $\Omega_1 \in [0.029, 0.14]$ sr.

The phosphor coating (prepared by sedimentation of phosphor grains on a substrate made by BK-7 glass, sealed with an aluminum layer of 100 nm) of type P43 (Gd_2O_2S:Tb) has an emission spectrum from 360 nm to 680 nm, peaked at 545 nm and a decay time of 1 ms. The efficiency may reach 700-800 photons per electron (with an electrostatic potential on the phosphor screen $V_F = 15$ kV). The back-illuminated CCD camera is cooled to $190 \div 210$ K by a Peltier element and has 1024x1024 pixels (each pixel being a 24 μm side square with a full well capacity of 3.5×10^5 electrons). An IR filter reduces the background light from the electron source.

The confining electrodes (with inner diameter of 90 mm), are aligned and mounted on an aluminum bar, attached to the reentrant flange; this structure can be inserted in the vacuum chamber sliding on some screws fixed under the bar. The other end of the bar is supported by an insert in the opposite flange. The potentials on the electrodes are controlled using a 8-channels waveform generator (time resolution 100 ns, voltage range ± 100 V, slew rate 300 V/μs).

The control and acquisition system is based on two personal computers (see Fig. 2): the first (PC1) is dedicated to the acquisition of the data from the CCD camera, the second (PC2) controls the settings of power supply and waveform generator, the logging of analog signals (e.g., the residual gas pressure) and the synchronization of the experiment. PC2 is equipped with five acquisition cards; up to 40 digital I/O's, 4 timers, 16 analog differential ± 10 V inputs and 4 analog outputs are provided; 6 RS232C ports and a GPIB bus are also available. Several analog interfaces between the machine and the acquisition system were built, solving specific tasks as, e.g, slow ramps (rise time ≥ 1 ms), and total charge detection. Slow ramps (power supply of the source filament and the accelerating voltage on the phosphor screen) are directly controlled by the PC2 analog output. A ground isolator between PC and power supply, given by a 4N25 optocoupler and scaling resistors, is introduced. To measure the number of trapped electrons, the aluminum layer on the phosphor screen is connected to an high-impedance low noise amplifier. This amplifier is also designed to work in differential mode for future applications (detection of diocotron waves).

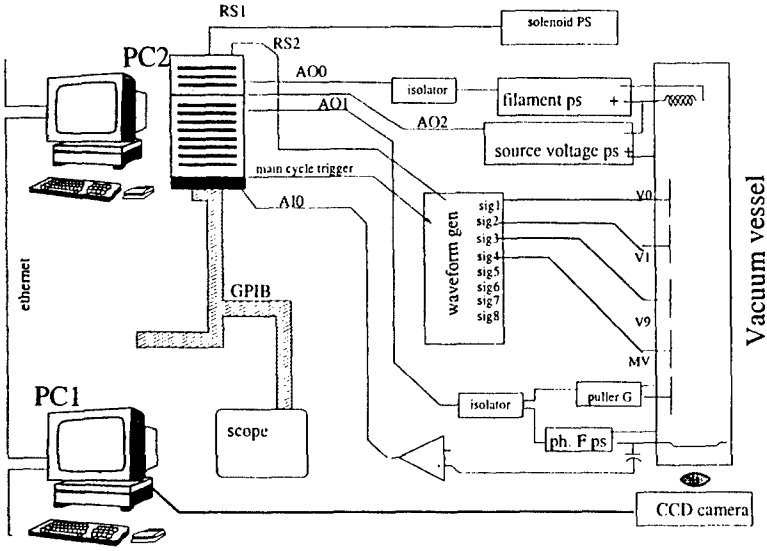

FIGURE 2. Scheme of the control and acquisition systems of the Eltrap machine.

ELECTRON SOURCES

The electron plasma is generated by a W/Th cathode arranged in a spiral shape [9], with diameter $D_f = 25$ mm. An extensive study of alternative sources (spiral carved disk of hot pressed W impregnated with Ba, and a W/Ce filament) has also been performed. The source is mounted inside a 44 mm long copper cup, which provides wire alignment and support and intercepts a fraction of the radiated heat; the wires are isolated by mullite tubes and connected to copper contacts, which are supported by macor isolators. The cup is attached to the electrode V_{ga} (see Fig. 1), thermally isolated from the bar by a macor spacer, so to distribute heat on a relatively large surface.

The generation of a relatively large plasma (diameter $2R_s \cong 60$ mm) with conventional filament sources proves difficult for the large amount of radiated heat P_m, which is related to the filament surface S_s, the filament current I_f and voltage V_f by

$$P_m = f_p \sigma S_s T_s^4 = \overline{I_f V_f} \tag{1}$$

where T_s is the working temperature, $f_p < 1$ is the relative emissivity (with geometrical corrections), σ is the Stefan-Boltzmann constant and the bar indicated time average. The emitted current I_s [10] is constrained by

$$I_s = f_i S_s A_r T_s^2 \exp[-\phi/(kT_s)] > \pi j_t R_s^2 \tag{2}$$

where $f_i \in [0.3, 1]$ is a numerical factor (determined by the geometry of the electrodes), ϕ is the work function of the material, $A_r = 120$ A K^{-2}cm^{-2} is the Richardson constant and $j \cong 10$ A m^{-2} is a target value. To obtain this target value $\phi < 2.5$ eV is necessary;

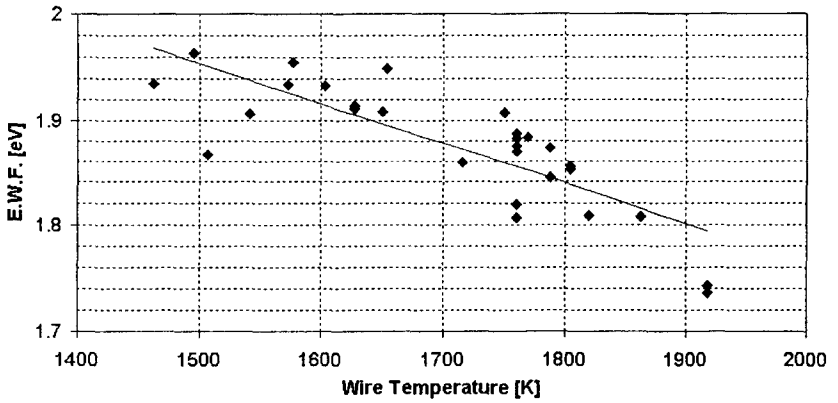

FIGURE 3. Test of a W/Ce spiral: thermionic emission work function. The solid line is the linear fit of the experimental data.

this is possible for hot pressed W with Ba impregnant ($\phi \cong 1.2 \pm 0.3$ eV), but the cost is quite high and machining can be troublesome.

Promising results of tests of a W/Ce source are reported in Fig. 3. A 1.5 turn spiral was prepared by carefully bending a 1 mm diameter W/Ce wire, with a total useful surface $S = 3.77$ cm^2. The emitted current I_s was measured as a function of the filament current I_f, in the range from 15 to 32 A (V_f ranged from 1 to 4.1 V). The temperature T was also measured by a pyrometer with a typical standard deviation error of ± 25 K; to reduce the error on T, the measured resistance of the filament R_f was scaled to $T = 1000$ K for every data point, using well-known tungsten resistivity data (24.9 $\mu\Omega$ cm at 1000 K and 56.7 $\mu\Omega$ cm at 2000 K); a resistance $R_f(T = 1000\ \text{K}) = (0.059 \pm 0.002)\ \Omega$ is obtained. The wire temperature is then computed for each data point, so that ϕ may be obtained from Eq. (2) ($f_i = 1$ in our experiment).

PERSPECTIVES

The basic ELTRAP configuration uses five cylindrical electrodes (out of twelve electrodes) for the inject-hold-dump cycle, controlled by the waveform generator. The plan of the experiments concerns studies on the formation and evolution of long lived coherent structures in a confined electron plasma (parameter range: B_0 = 200-2000 G, charge Q = 10-600 nC, plasma length 20-80 cm). In the future the device will be also used to investigate the spatial disuniformities (transverse and axial) of an electron beam, due to collective effects. This is of interest for beam dynamics, being one of the most important causes of emittance growth in high brilliance beams (for FEL). To this aim, a moving phosphor equipped telescope will be possibly installed, for 3D analysis.

ACKNOWLEDGMENTS

The authors are grateful to F. C. Driscoll, J. Fajans, A. Cass and K. S. Fine for very valuable discussions and suggestions during the development of the ELTRAP project.

This work has been supported by the Italian Ministry of Education and Scientific Research, the National Institute for the Physics of Matter (I.N.F.M.) and the National Institute of Nuclear Physics (I.N.F.N.).

REFERENCES

1. D. H. E. Dubin and T. M. O'Neil, Rev. Mod. Phys. **71**, 87 (1999).
2. K. S. Fine, W. G. Flynn, A. C. Cass, and C. F. Driscoll, Phys. Rev. Lett. **75**, 3277 (1995).
3. D. Durkin and J. Fajans, Phys. Rev. Lett. **85**, 4052 (2000).
4. M. Romé, M. Brunetti, F. Califano, F. Pegoraro, and R. Pozzoli, Phys. Plasmas **7**, 2856 (2000).
5. M. Amoretti, D. Durkin, J. Fajans, R. Pozzoli, and M. Romé, Phys. Plasmas **8**, 3865 (2001).
6. R. Pozzoli and D. Ryutov, Electromagnetic Waves and Electronic Systems **3**, 12 (1998).
7. C. F. Driscoll, J. H. Malmberg, and K. S. Fine, Phys. Rev. Lett. **60**, 1290 (1988).
8. X. P. Huang, K. S. Fine, and C. F. Driscoll, Phys. Rev. Lett. **74**, 4424 (1995).
9. J. M. Kriesel and C. F. Driscoll, Phys. Plasmas **5**, 1265 (1998).
10. G. A. Haas, in *Methods of experimental physics*, vol. 4A, p. 1 (Academic Press, New York, 1967).